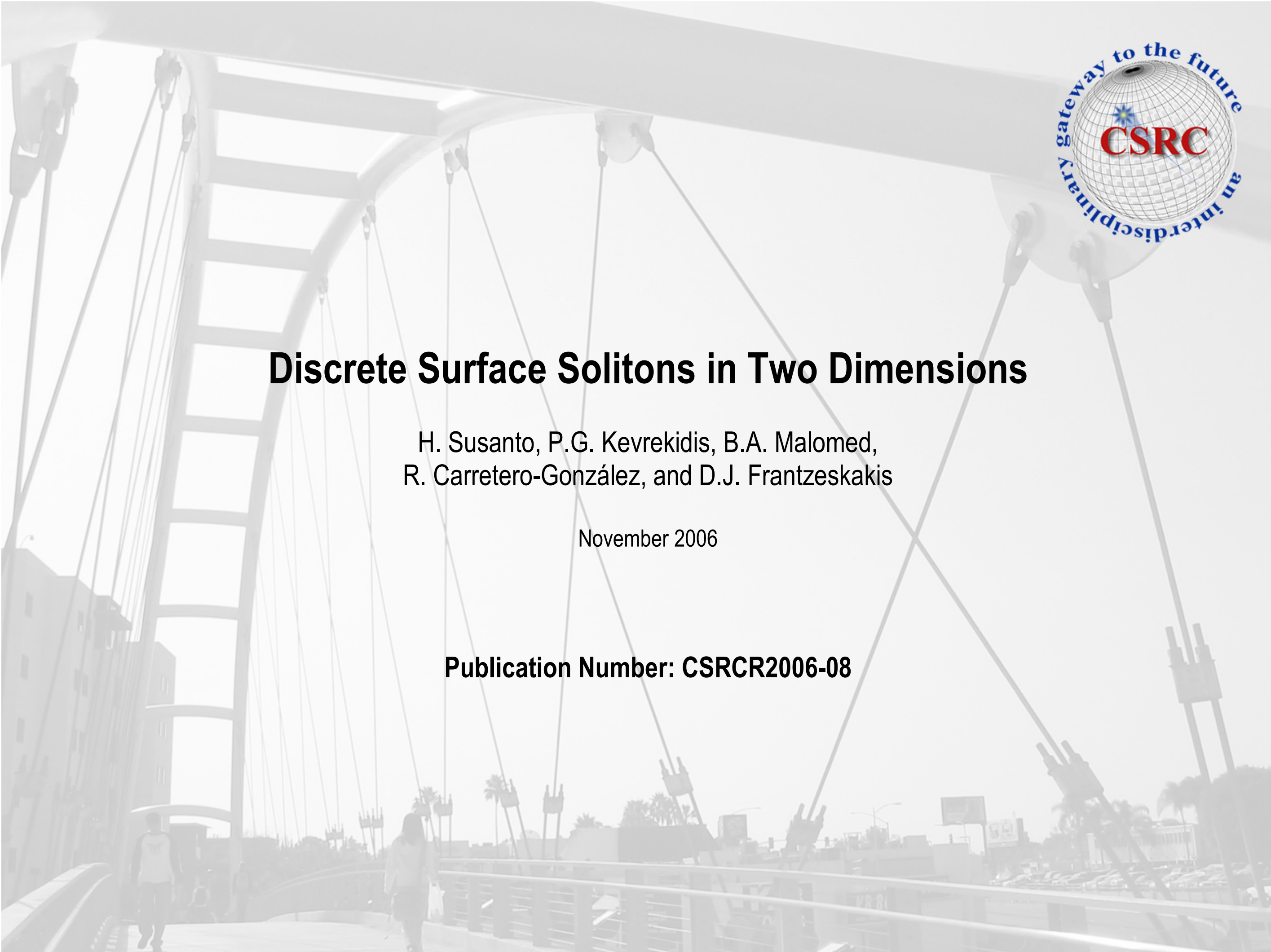

Discrete Surface Solitons in Two Dimensions

H. Susanto, P.G. Kevrekidis, B.A. Malomed,
R. Carretero-González, and D.J. Frantzeskakis

November 2006

Publication Number: CSRCR2006-08

Computational Science &
Engineering Faculty and Students
Research Articles

Database Powered by the
Computational Science Research Center
Computing Group

COMPUTATIONAL SCIENCE & ENGINEERING

SAN DIEGO STATE UNIVERSITY

Computational Science Research Center
College of Sciences
5500 Campanile Drive
San Diego, CA 92182-1245
(619) 594-3430

Discrete surface solitons in two dimensions

H. Susanto,[1] P. G. Kevrekidis,[1] B. A. Malomed,[2] R. Carretero-González,[3] and D. J. Frantzeskakis[4]

[1]*Department of Mathematics and Statistics, University of Massachusetts, Amherst MA 01003-4515, USA*
[2]*Department of Interdisciplinary Studies, School of Electrical Engineering, Faculty of Engineering, Tel Aviv University, Tel Aviv 69978, Israel*
[3]*Nonlinear Dynamical Systems Group*, Department of Mathematics and Statistics, and Computational Science Research Center†, San Diego State University, San Diego CA, 92182-7720, USA*
[4]*Department of Physics, University of Athens, Panepistimiopolis, Zografos, Athens 15784, Greece*

(Dated: Submitted to *Phys. Rev. E*, November 2006)

We investigate fundamental localized modes in 2D lattices with an edge (surface). The interaction with the edge expands the stability area for ordinary solitons, and induces a difference between dipoles oriented perpendicular and parallel to the surface. On the contrary, lattice vortices cannot exist too close to the border. Furthermore, we show, analytically and numerically, that the edge stabilizes a novel species of localized patterns, which is entirely unstable in the uniform lattice, namely, a "horseshoe" soliton, whose "skeleton" consists of three lattice sites. Unstable horseshoes transform themselves into a pair of ordinary solitons.

PACS numbers: 05.45.Yv, 03.75.-b, 42.65.Tg

I. INTRODUCTION AND THE MODEL

Solitons on surfaces of fluids [1], solids [2], and plasmas [3] have been the subject of numerous experimental and theoretical studies. Recently, a new implementation of surface solitary waves was proposed [4] and experimentally realized [5] in nonlinear optics, in the form of *discrete* localized states supported at the edge of a semi-infinite array of nonlinear waveguides. Two-component surface solitons were analyzed too [6], and it was predicted that solitons may be supported at an edge of a discrete chain by a nonlinear impurity [7]. Parallel to that, surface solitons of the gap type were predicted [8] and created in an experiment [9] at an edge of a waveguiding array built into in a self-defocusing continuous medium. Very recently, the experimental creation of discrete surface solitons supported by the quadratic nonlinearity was reported as well [10]. In these cases, the solitons are one-dimensional (1D) objects. In Ref. [11], a two-dimensional (2D) medium with saturable nonlinearity was considered, with an embedded square lattice, that has a jump at an internal interface; in that setting, stable asymmetric vortex solitons crossing the interface were predicted, as a generalization of discrete vortices on 2D lattices [12] and vortex solitons supported by optically induced lattices in photorefractive media [13]. Solitons supported by a nonlinear defect at the edge of a 2D lattice were considered too [14].

The search for surface solitons in lattice settings is a natural issue, as, in any experimental setup, the lattice inevitably has an edge. In this paper, we report new results for discrete surface solitons in semi-infinite 2D lattices. First, we consider the effect of the surface on fundamental lattice solitons, and two types of dipoles, oriented perpendicular or parallel to the surface. Then, we introduce a novel species of localized states, a *horseshoe soliton*, in the form of an arc abutting upon the lattice's edge. The existence, and especially the stability, of such a localized mode is a nontrivial issue, as attempts to find a "horseshoe" in continuum media with imprinted lattices and an internal interface (such as those considered in Ref. [11]) have produced negative results [15]. We find that, in the semi-infinite discrete medium, the horseshoes do exist near the lattice edge, and have their stability region. For comparison, we also construct a family of localized patterns of the same type in the uniform lattice [which, incidentally, is a kind of a stationary localized solutions of the 2D discrete nonlinear Schrödinger (DNLS) equation that has not been studied previously]. In particular, we find that this family of solutions is *completely unstable* in the infinite uniform lattice (the one without an edge), which stresses the nontrivial character of the surface-abutting horseshoes, that may be made stable by the interaction with the lattice edge.

The model of a semi-infinite 2D array of optical waveguides with a horizontal edge, that we consider here as a physically relevant representative of the semi-infinite lattices in two dimensions, is based on the DNLS equation for amplitudes $u_{m,n}(z)$ of the electromagnetic waves in the guiding cores, with z the propagation distance:

$$i\frac{du_{m,n}}{dz} + C(u_{m+1,n} + u_{m-1,n} + u_{m,n+1} + u_{m,n-1} - 4u_{m,n}) + |u_{m,n}|^2 u_{m,n} = 0, \quad (1)$$

for $n \geq 2$ and all m, where C is the coupling constant, the corresponding coupling length in the waveguide array, C^{-1}, usually being, in physical units, on the order

*URL: http://nlds.sdsu.edu/
†URL: http://www.csrc.sdsu.edu/

of a few millimeters. At the surface row, which corresponds to $n = 1$ in Eq. (1), the equation is modified by dropping the fourth term in the combination of linear terms in Eq. (1) (cf. the 1D model in Refs. [5]), $u_{m,0} = 0$, as there are no waveguides at $n \leq 0$. Note that, despite the presence of the edge, Eq. (1) admits the usual Hamiltonian representation, and conserves the total power (norm) , $P = \sum_{m=-\infty}^{+\infty} \sum_{n=1}^{+\infty} |u_{m,n}|^2$. It is worth mentioning that there exists another physical realization of the same model: The DNLS Eq. (1) describes, in the mean-field approximation, the dynamics of a Bose-Einstein condensate (BEC) trapped in a strong 2D optical lattice [16] (the latter is a periodic potential induced by the interference of counter propagating pairs of coherent laser beams illuminating the condensate). In such a case, $u_{m,n}$ is the condensate wavefunction, and C is the tunneling rate between adjacent wells of the optical lattice. Notice that in the latter context a sharp edge can be easily created by means of a repelling (blue-detuned) light sheet bordering the condensate.

Stationary solutions to Eq. (1) will be looked for as $u_{m,n} = e^{ikz} v_{m,n}$, where the wavenumber k may be scaled to 1, once the coupling coefficient, C, is kept as an arbitrary parameter. The above stationary solution obeys the equation

$$\begin{aligned}(1 \; - \; |v_{m,n}|^2) v_{m,n} - C(v_{m,n+1} + v_{m,n-1} \\ + \; v_{m+1,n} + v_{m-1,n} - 4v_{m,n}) = 0,\end{aligned} \tag{2}$$

with the same modification as above at $n = 1$.

The rest of the paper is organized as follows: In section II, we will report results of an analytical approximation for the shape and stability of dipoles and "horseshoes", valid for a weakly coupled lattice (for small C). This will be followed by presentation of corresponding numerical results. In section III we will briefly consider the interaction of vortices with the lattice's edge and, finally, in section IV we will summarize our findings.

II. PERTURBATIVE ANALYSIS

Analytical results can be obtained for small C, starting from the anti-continuum (AC) limit, $C = 0$ (see Ref. [17] and references therein). In this case, solutions to Eq. (2) may be constructed as a perturbative expansion

$$v_{m,n} = \sum_{k=0}^{\infty} C^k v_{m,n}^{(k)}.$$

In the AC limit proper, the *seed solution*, $v_{m,n}^{(0)}$, is zero except at a few *excited sites*, which determine the configuration. Of course, a great variety of seed solutions can be formally constructed in the AC limit proper. A nontrivial issue is to identify ones that may be continued to *finite values* of C as *stable solutions*. As concerns the experimental realization, the necessary set of sites can be easily excited selectively, by focusing the input laser beam(s) on them, as shown, for instance, in experimental studies of interactions between discrete solitons in waveguide arrays [18].

We will develop an analytical approach to the study of the following configurations: (A) a fundamental surface soliton, seeded by a single excited site, $v_{1,1}^{(0)} = 1$ (the first subscript 1 denotes the soliton's location in the horizontal direction), (B) surface dipoles, oriented perpendicular (B1) or parallel (B2) to the edge, each seeded at two sites,

$$\left\{ v_{0,1}^{(0)}, v_{0,2}^{(0)} \right\} = \{-1, 1\}\,, \text{ or } \left\{ v_{0,1}^{(0)}, v_{1,1}^{(0)} \right\} = \{-1, 1\}\,, \tag{3}$$

and (C) the "horseshoe" three-site-seeded structure,

$$\left\{ v_{1,1}^{(0)}, v_{0,2}^{(0)}, v_{-1,1}^{(0)} \right\} = \left\{ e^{i\theta_{1,1}}, e^{i\theta_{0,2}}, e^{i\theta_{-1,1}} \right\}, \tag{4}$$

with $\theta_{1,1} = 0$, $\theta_{0,2} = \pi$, $\theta_{-1,0} = 2\pi$. As concerns stable dipole states on the infinite lattice, they were predicted in Ref. [19], and later observed experimentally in a photonic lattice induced in a photorefractive crystal [20]. All the above seed configurations are real; in particular, the horseshoe may, in principle, be regarded as a truncated *quadrupole*, which is a real solution too [21].

At small $C > 0$, it is straightforward to calculate corrections to the stationary states at the first order in C. Then, the stability of each state is determined by a set of eigenvalues, λ, which are expressed in terms of eigenvalues μ of the corresponding *Jacobian matrix*, to be derived in a perturbative form, $\mathcal{M} = \sum_{k=0}^{\infty} C^k \mathcal{M}_k$, from the linearized equations for small perturbations around a given stationary state [17]. Because the present system is a Hamiltonian one, the stability condition is $\mathrm{Re}(\lambda) = 0$ for all λ (if λ is an eigenvalue, so also are $-\lambda$, $\lambda^\star$ and $-\lambda^\star$, hence only imaginary λ does not imply instability).

For the dipole and horseshoe configurations, which were denoted above as (B1,B2) and (C), respectively, the calculations result in

$$\mathcal{M}^{(\mathrm{B})} \;=\; C \begin{pmatrix} -1 & 1 \\ 1 & -1 \end{pmatrix} + \mathcal{O}\left(C^2\right),$$

$$\mathcal{M}^{(\mathrm{C})} \;=\; C^2 \begin{pmatrix} -4 & 2 & 2 \\ 2 & -1 & -1 \\ 2 & -1 & -1 \end{pmatrix} + \mathcal{O}\left(C^3\right) \tag{5}$$

[the matrices for (B1) and (B2) coincide, at this order]. From here, we obtain *stable* eigenvalues, at the lowest nontrivial order, $\lambda_1^{(\mathrm{B})} = 0, \lambda_2^{(\mathrm{B})} = \pm 2\sqrt{C} i + \mathcal{O}(C)$, and $\lambda_1^{(\mathrm{C})} = 0, \lambda_2^{(\mathrm{C})} = \mathcal{O}\left(C^2\right), \lambda_3^{(\mathrm{C})} = \pm 2\sqrt{3} C i + \mathcal{O}\left(C^2\right)$. Both for the dipoles and horseshoe, one eigenvalue is exactly zero, corresponding to the Goldstone mode generated by the phase invariance of the underlying DNLS equation. As for eigenvalue $\lambda_2^{(\mathrm{C})}$, it becomes different from zero at order $\mathcal{O}\left(C^2\right)$, and, as shown below, it plays a critical role in determining the stability of the horseshoe structure.

We do not consider the fundamental soliton, (A), here, as its destabilization mechanism is different (and requires

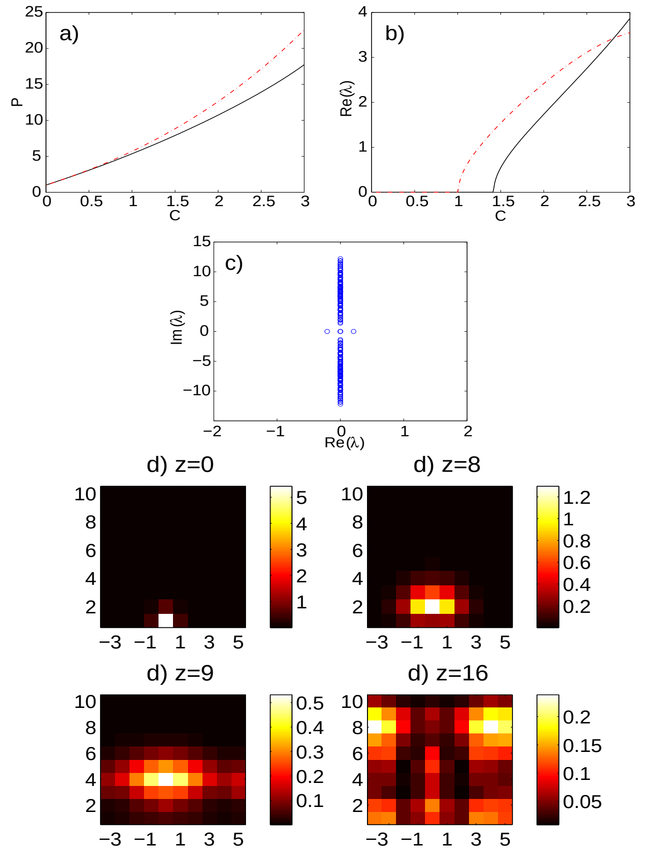

FIG. 1: (Color online) Dynamical features of the fundamental lattice-surface soliton. Fundamental characteristics of the soliton family, *viz.* a) the soliton's norm P, and b) the real part of the critical stability eigenvalue, versus the lattice coupling constant, C. For comparison, the dash-dotted lines show respective quantities for the fundamental soliton in the infinite lattice. The instability is due to an eigenvalue pair bifurcating from the edge of the phonon band, that eventually hits the origin of the spectral plane and thus becomes real. c) Linear-stability spectrum of the fundamental soliton. d) Snapshots of its evolution (contour plots of $|u_{m,n}|^2$), slightly above the instability threshold (at $C = 1.43$).

a different analysis) from that of the dipoles and horseshoes; in particular, the critical eigenvalues bifurcate not from zero, but from the edge of continuous spectrum (see below).

To examine the existence and stability of the above configurations numerically, we start with the fundamental onsite soliton at the surface, (A). Basic results for this state are displayed in Fig. 1. At $C = 0$, there is a double zero eigenvalue due to the phase invariance. For small $C > 0$, this is the only eigenvalue of the linearization near the origin of the spectral plane $(\mathrm{Re}(\lambda), \mathrm{Im}(\lambda))$. As C increases, one encounters a critical value, at which an additional (but still marginally stable) eigenvalue bifurcates from the edge of the continuous spectrum, as mentioned above. With the further increase of C, this eigenvalue hits the origin of the spectral plane, which gives birth to an *unstable* eigenvalue pair, with $\mathrm{Re}(\lambda) \neq 0$, see panel c) in Fig. 1. The corresponding instability occurs at $C > 1.41$ (the results reported here have been obtained for lattices of size 10×10, but it has been verified that a similar phenomenology persists for larger lattices, up to 25×25). For comparison, we also display in Fig. 1, by a dashed-dotted line, the critical unstable eigenvalue for a fundamental soliton on the uniform lattice (in other words, for a soliton sitting far from the lattice's edge), which demonstrates that the interaction with the edge leads to a conspicuous *expansion of the stability interval* of the fundamental soliton. This result may be understood, as the instability of the fundamental soliton emerges as one approaches the continuum limit; 2D solitons in the continuum NLS equation are well-known to be unstable due to the possibility of the critical collapse in this case. On the other hand, a discrete fundamental soliton located near the surface interacts with fewer neighboring sites, hence it approaches the continuum limit slower, in comparison with its counterpart in the infinite lattice.

Development of the instability of the fundamental surface soliton (in the case when it is unstable) was examined in direct simulations of Eq. (1). As seen in panel d) of Fig. 1, in this case the soliton moves away from the lattice's edge, expanding into an apparently disordered state (lattice radiation). This outcome of the instability development is understandable, as, at these values of the parameters, stable localized state exists, near the surface or in the bulk of the lattice, where the fundamental soliton is still more unstable.

Next, in Fig. 2 we present results for the vertical and horizontal dipoles, (B1) and (B2), seeded as per Eq. (3). At $C = 0$, the spectrum of perturbation eigenmodes around the dipole contains two pairs of zero eigenvalues, one of which becomes finite (remaining stable, i.e., imaginary) at $C > 0$, as shown above in the analytical form. Our numerical findings reveal that, in compliance with the analytical results, the dipoles of both types give rise to virtually identical finite eigenvalues [hence only one eigenvalue line is actually seen in panel d) of Fig. 2]. As shown in panel e) of Fig. 2, both dipoles lose their stability simultaneously, at $C \approx 0.15$. Continuing the computations past this point, we conclude that the vertical and horizontal dipoles become different when C attains values ~ 1. Eventually, the (already unstable) vertical configuration, (B1), disappears in a saddle-node bifurcation at $C \approx 2.17$, while its horizontal counterpart, (B2), persists through this point. Furthermore, there is a critical value of C at which an eigenvalue bifurcates from the edge of the continuous spectrum. Eventually, this bifurcating eigenvalue crosses the origin of the spectral plane, giving rise to an unstable eigenvalue pair, with $\mathrm{Re}(\lambda) \neq 0$. The value of C at which this secondary instability sets in is essentially smaller for (B1), i.e., $C \approx 1.55$, than $C \approx 2.61$ for (B2). We thus conclude that the horizontal dipole, (B2), is, generally, more robust than its vertical counterpart, (B1), as concerns both its existence and stability. This conclusion seems natural, as the proximity to the

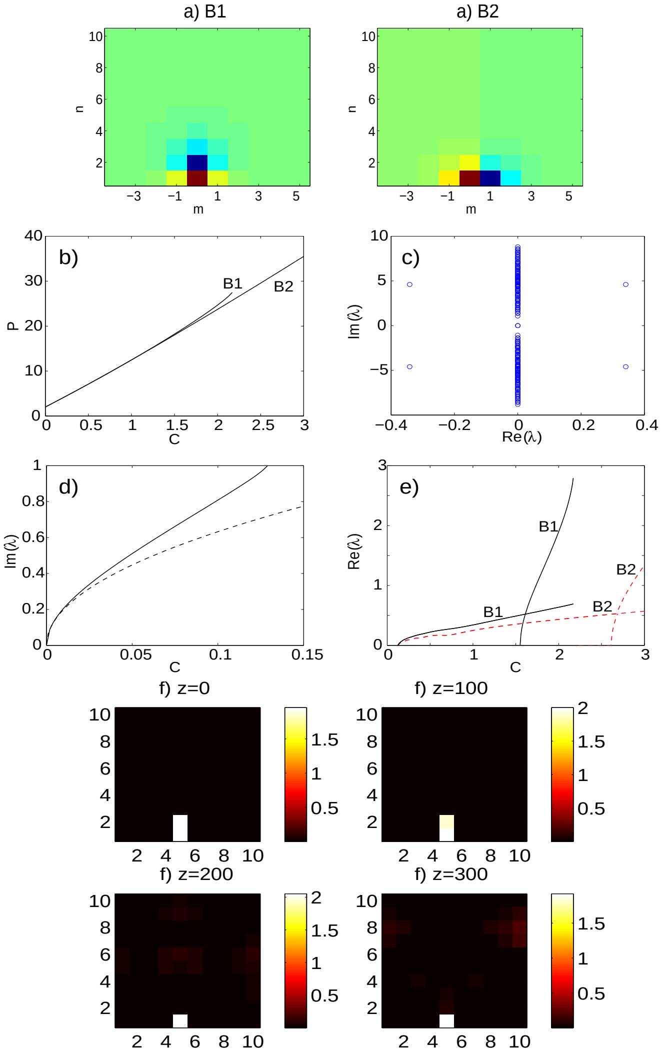

FIG. 2: (Color online) a) Vertical (B1) and horizontal (B2) dipoles for $C = 1$. Their respective norms are depicted in panel b). The imaginary and real part of the critical stability eigenvalue, versus the lattice coupling constant, C, are displayed in panels d) and e) respectively. The vertical dipole (B1) disappears via a saddle-node bifurcation at $C \approx 2.17$. Panel d) depicts the eigenvalue bifurcating from zero at $C = 0$, the dashed line being the analytical approximation described in the text, i.e., $(\mathrm{Im}(\lambda))^2 = 4C$. Panel e) shows the onset of instability in the (B1) (solid lines) and (B2) (dashed lines) dipoles, as found from numerical computations. Panels c) and f) show, respectively, the spectrum of the stability eigenvalues and nonlinear evolution of an unstable vertical dipole for $C = 0.2$.

lattice edge stabilizes the fundamental soliton, as shown above, and in the horizontal configuration the two fundamental solitons that constitute the dipole are located closer to the border.

Nonlinear evolution of unstable dipoles was examined in direct simulations as well. As seen in the example [for the configuration (B1)] shown in panels f) of Fig. 2, the instability transforms them into fundamental solitons.

Proceeding to the novel discrete-soliton species (C),

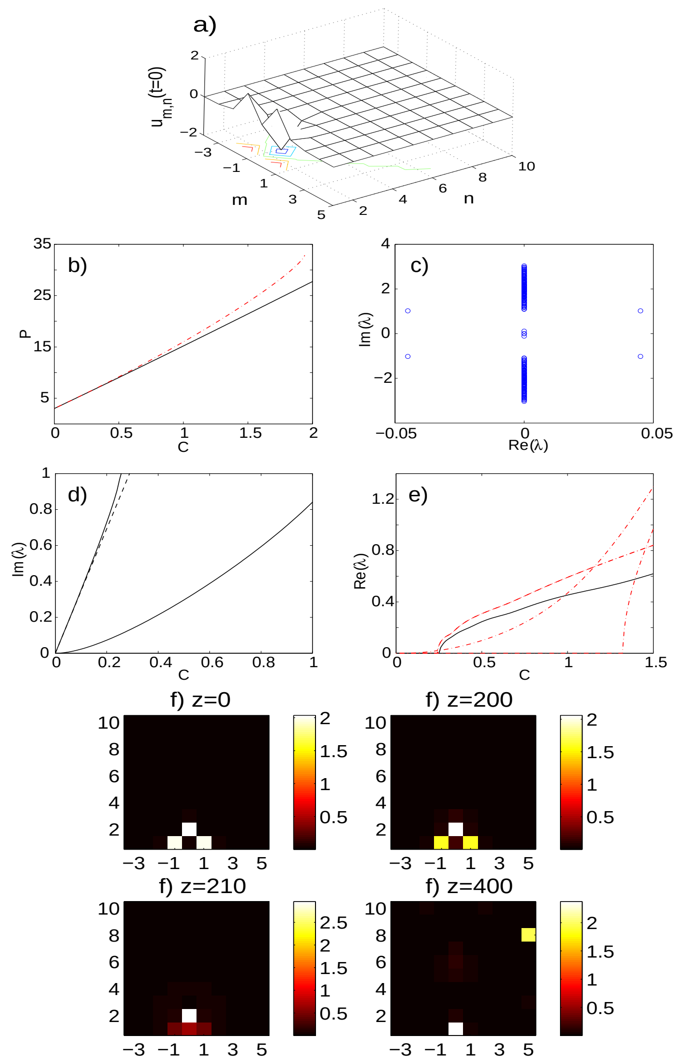

FIG. 3: (Color online) The same as Fig. 2 for the “horseshoe” configuration, seeded at $C = 0$ as per Eq. (4), i.e., as a truncated “quadrupole”. Panel a) shows an example of the state. The solid curves in the panels d) and e) display the imaginary an real parts of critical stability eigenvalues [the dashed line in d) presents the analytical approximation for the imaginary part, see in the text]. For comparison, the red dash-dotted lines in e) show the same characteristics for a family of horseshoe solitons created in the uniform lattice (without the edge). It is seen that the latter family is *completely unstable*, while the horseshoe trapped at the edge of the lattice has a well-defined stability region. Panels c) and f) present, respectively, the linear instability spectrum of the horseshoe at $C = 0.26$, and its (numerically simulated) evolution due to the instability.

namely the horseshoe, we note that, because it is seeded at three sites in the AC limit, there are three pairs of zero eigenvalues at $C = 0$. Above, it was shown analytically that one pair of these eigenvalues becomes finite at order $\mathcal{O}(C)$, and another at $\mathcal{O}(C^2)$. These analytical results are continued by means of numerical computations (see Fig. 3). It was found that the first pair remains stable (imaginary) until it collides with the edge of the continuous spectrum, which happens at $C \approx 0.25$ [see panel e) of Fig. 3]. As mentioned above, the second eigenvalue pair, bifurcating from zero at order $\mathcal{O}\left(C^2\right)$, is critical for the stability of configuration (C) at $C \to 0$. The numerical results show that this pair bifurcates into a *stable* one, hence, as shown in Fig. 3, the horseshoe remains stable up to the above-mentioned value, $C \approx 0.25$, at which the first pair suffers a bifurcation into an unstable one, due to the collision with the continuous band.

To understand the stabilizing effect of the surface on the horseshoes, it is relevant to compare them to their counterparts that may be found in the infinite lattice. Indeed, again starting with the AC seed taken as per Eq. (4) but far from the lattice's edge, we have created stationary structures similar to the horseshoe. By themselves, they present a novel family of localized solutions to the DNLS equation in 2D. However, this *entire family* turns out to be unstable (unlike the ordinary quadrupoles that may be stable [21]), through the following mechanism: the $\mathcal{O}(C^2)$ eigenvalue pair, bifurcating from zero at $C = 0$, immediately becomes real in this case, see the corresponding parabolic dashed-dotted line in panel e) of Fig. 3. We stress that, unlike the above example of the stabilization of the fundamental soliton by its proximity to the lattice edge, the dependence of the horseshoe's stability on the border is crucial, as it may never be stable in the infinite lattice.

Panels f) of Fig. 3 exemplify the evolution of the horseshoe when it is unstable. We observe that the unstable horseshoe splits into a pair of two fundamental solitons, one trapped at the surface and one found deeper inside the lattice.

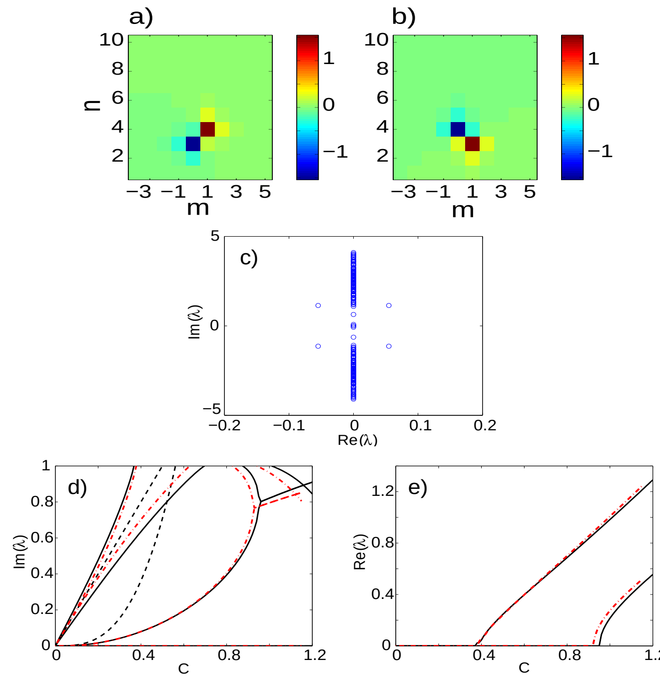

FIG. 4: (Color online) The *supersymmetric* vortex cell seeded as per Eq. (7). Panels a) and b) show, respectively, the real and imaginary parts of the solution and panel c) the (in)stability spectrum of small perturbations around it for $C = 0.4$. Panels d) and e) display imaginary and real parts of the stability eigenvalues versus C. The solid and dashed lines show numerical and analytical results for small C. For comparison, red dashed-dotted lines depict the same numerically found characteristics for a supersymmetric vortex on the infinite lattice.

III. EFFECTS OF THE LATTICE SURFACE ON THE EXISTENCE OF VORTICES

In spite of the stabilization effects reported above, the lattice edge may also act in a different way, impeding the existence of localized solutions of other types. As an interesting example, we consider the so-called *supersymmetric lattice vortex* [17] attached to the edge, i.e., one with the vorticity ($S = 1$) equal to the size of the square which seeds the vortex at $C = 0$ through the following set of four excited sites, cf. Eq. (4):

$$\left\{v_{0,1}^{(0)}, v_{1,1}^{(0)}, v_{1,2}^{(0)}, v_{0,2}^{(0)}\right\} = \left\{e^{i\theta_{0,1}}, e^{i\theta_{1,1}}, e^{i\theta_{1,2}}, e^{i\theta_{0,2}}\right\}, \quad (6)$$

with $\theta_{0,1} = 0$, $\theta_{1,1} = \pi/2$, $\theta_{1,2} = \pi$, and $\theta_{0,2} = 3\pi/2$ (unlike the above configurations, this one is complex). While supersymmetric vortices exist in uniform lattices (including anisotropic ones), and have their own stability regions there [17, 22], numerical analysis shows that the localized state seeded as per Eq. (6) in the model with the edge *cannot* be continued to $C > 0$ (which illustrates the above statement that arbitrary patterns created in the AC limit do not continued to finite C, and the continuation selects only truly existing lattice solutions). In fact, we have found that, to create such a state at finite C, we need to seed it, at least, *two sites away* from the edge, i.e., as

$$\left\{v_{0,3}^{(0)}, v_{1,3}^{(0)}, v_{1,4}^{(0)}, v_{0,4}^{(0)}\right\} = \left\{e^{i\theta_{0,3}}, e^{i\theta_{1,3}}, e^{i\theta_{1,4}}, e^{i\theta_{0,4}}\right\}, \quad (7)$$

where the set on the right-hand side is a translated version of that of Eq. (6). Numerically found stability eigenvalues for this structure are presented in Fig. 4, along with the analytical approximation, obtained, for small C, by means of the same method as above. In all, there are four pairs of analytically predicted eigenvalues near the spectral-plane origin (given the four initially seeded sites of the configuration). More specifically, these are: $\lambda = 0$ (it corresponds to the Goldstone mode associated with the phase invariance), $\lambda = \pm 2iC$ (a double eigenvalue pair), and $\lambda = \pm\sqrt{32}C^3 i$ (a higher-order pair). As seen in the figure, the distance of two sites from the boundary is sufficient to make the behavior of the supersymmetric lattice vortex sufficiently close to that in the infinite lattice and to render it stable.

IV. CONCLUSION

This work demonstrates that properties of localized modes in the 2D lattice with an edge may be drastically different from well-known features in the uniform lattice. In particular, the edge helps to increase the stability region for the fundamental solitons, and induces a difference between dipoles oriented perpendicular and parallel to the lattice's border, making the latter ones more robust. On the other hand, an opposite trend was demonstrated for supersymmetric vortices, which cannot be created too close to the border. Most essentially, the edge stabilizes a new species of discrete solitons which is entirely unstable in the uniform lattice, the "horseshoes". The stabilizing effect exerted by the edge on the fundamental solitons, horizontal dipoles, and horseshoes suggest new possibilities for experiments in 2D arrays of nonlinear optical waveguides, as well as in BEC trapped in a deep 2D optical lattice. In particular, a straightforward estimate shows that the longest dimensionless propagation distance, $z \lesssim 400$, for which the simulations were run, to demonstrate the evolution of unstable modes in full detail and show their clear distinction from the stable ones, corresponds to the waveguide length $\lesssim 4$ cm, which is quite possible in the current experiments [18].

Natural issues for further consideration are horseshoes of a larger size (the present work was dealing with the most compact ones), and counterparts of such localized modes in 3D lattices near the edge – possibly, in the form of "bells" abutting on the surface. In the 3D lattice, one can also consider solitons in the form of vortex rings or cubes [23] set parallel to the border. In this connection, it is relevant to note that the 3D version of the DNLS equation does not apply to the guided-wave propagation in optics, but it can be realized in terms of BEC loaded in a strong 3D optical lattice, see Ref. [23] and references therein.

P.G.K. gratefully acknowledges support from NSF-DMS-0204585, NSF-CAREER. R.C.G. and P.G.K. also acknowledge support from NSF-DMS-0505663.

[1] R. K. Dodd, J. C. Eilbeck, J. D. Gibbon, and H. C. Morris. *Solitons and nonlinear wave equations* (Academic Press, London, 1982).

[2] G. Maugin. *Nonlinear Waves in Elastic Crystals* (Oxford University Press: Oxford, 2000).

[3] L. Stenflo, Physica Scripta **T63**, 59 (1996).

[4] K. G. Makris, S. Suntsov, D. N. Christodoulides, G. I. Stegeman, and A. Hache, Opt. Lett. **30**, 2466 (2005); M. I. Molina, R. A. Vicencio, and Y. S. Kivshar, Opt. Lett. **31,** 1693 (2006).

[5] S. Suntsov, K. G. Makris, D. N. Christodoulides, G. I. Stegeman, A. Haché, R. Morandotti, H. Yang, G. Salamo, and M. Sorel, Phys. Rev. Lett. **96**, 063901 (2006).

[6] I. L. Garanovich, A. A. Sukhorukov, Y. S. Kivshar, and M. Molina, Opt. Express **14**, 4780 (2006).

[7] M. I. Molina, Phys. Rev. B **71**, 035404 (2005); *ibid.* **73**, 014204 (2006).

[8] Y. V. Kartashov, L. Torner and V. A. Vysloukh, Phys. Rev. Lett. **96**, 073901 (2006); W. H. Chen, Y. J. He, and H. Z. Wang, Opt. Exp. **14**, 11271 (2006).

[9] C. R. Rosberg, D. N. Neshev, W. Krolikowski, A. Mitchell, R. A. Vicencio, M. I. Molina, and Y. S. Kivshar, Phys. Rev. Lett. **97**, 083901 (2006).

[10] G. A. Siviloglou, K. G. Makris, R. Iwanow, R. Schiek, D. N. Christodoulides, G. I. Stegeman, Y. Min, and W. Sohler, Opt. Exp. **14**, 5508 (2006).

[11] Y. V. Kartashov, A. A. Egorov, V. A. Vysloukh, and L. Torner, Opt. Express **14**, 4049 (2006).

[12] B. A. Malomed and P. G. Kevrekidis, Phys. Rev. E **64**, 026601 (2001).

[13] D. N. Neshev, T. J. Alexander, E. A. Ostrovskaya, and Y. S. Kivshar, H. Martin, I. Makasyuk, and Z. Chen, Phys. Rev. Lett. **92**, 123903 (2004); J. W. Fleischer, G. Bartal, O. Cohen, O. Manela, M. Segev, J. Hudock, and D. N. Christodoulides, Phys. Rev. Lett. **92**, 123904 (2004).

[14] M. I. Molina, Phys. Rev. B **74**, 045412 (2006).

[15] Y. V. Kartashov, private communication.

[16] A. Trombettoni and A. Smerzi, Phys. Rev. Lett. **86**, 2353 (2001); G. L. Alfimov, P. G. Kevrekidis, V. V. Konotop, and M. Salerno, Phys. Rev. E **66**, 046608 (2002).

[17] D. E. Pelinovsky, P. G. Kevrekidis and D. J. Frantzeskakis, Physica D **212**, 20 (2005).

[18] J. Meier, G. I. Stegeman, Y. Silberberg, R. Morandotti, and J. S. Aitchison, Phys. Rev. Lett. 93, 093903 (2004); Y. Linzon, Y. Sivan, B. Malomed, M. Zaezjev, R. Morandotti, *ibid.* **97**, 193901 (2006).

[19] P. G. Kevrekidis, B. A. Malomed, and A. R. Bishop, J. Phys. A: Math. Gen. **34**, 9615 (2001).

[20] J. Yang, I. Makasyuk, A. Bezryadina, and Z. G. Chen, Stud. Appl. Math. **113**, 389 (2004); Z. G. Chen, H. Martin, E. D. Eugenieva, J. J. Xu, and J. K. Yang, Opt. Express **13**, 1816 (2005).

[21] P. G. Kevrekidis, B. A. Malomed, Z. Chen, and D. J. Frantzeskakis, Phys. Rev. E **70**, 056612 (2004); H. Sakaguchi and B. A. Malomed, Europhys. Lett. **72**, 698 (2005).

[22] P. G. Kevrekidis, D. J. Frantzeskakis, R. Carretero-González, B. A. Malomed, and A. R. Bishop, Phys. Rev. E **72**, 046613 (2005).

[23] P. G. Kevrekidis, B. A. Malomed, D. J. Frantzeskakis and R. Carretero-González, Phys. Rev. Lett. **93**, 080403 (2004); R. Carretero-González, P. G. Kevrekidis, B. A. Malomed and D. J. Frantzeskakis, *ibid.* **94**, 203901 (2005).